*Journal of Applied Mechanics and Technical Physics, Vol. 49, No. 6, pp. 946–956, 2008*

# MATHEMATICAL SIMULATION OF CONJUGATE MIXED CONVECTION IN A RECTANGULAR REGION WITH A HEAT SOURCE

**G. V. Kuznetsov**[1] **and M. A. Sheremet**[2]

UDC 669.86:536.21

*Conjugate convective-conductive heat transfer in a rectangular region with forced flow and a heat source is simulated numerically. Distributions of the thermal and hydrodynamic characteristics of the flow regimes studied are obtained. The evolution of the process analyzed is shown.*

**Key words:** *conjugate heat transfer, mixed convection, locally concentrated heat source, rectangular region, laminar flow.*

**Introduction.** The joint analysis of convection in a gas cavity and conductive heat transfer in solid blocks is of great theoretical significance [1, 2] and applied significance [3–13]. Recently, there has been increased interest in this problem [2–13] due to the possibility of using the theory of conjugate heat transfer in modern and promising technological systems. Results have been obtained that describe various flow regimes and configurations of solution regions. Lykov [1] considered a class of conjugate problems of convective heat transfer (simple geometry, external boundary conditions mainly of the first and second kind), analyzed conditions under which the conjugate formulation is the most correct, and found significant singularities of this class of problems. Great attention has been given to the problem of formulating conjugate problems. Liaqat and Baytas [2] performed numerical simulations of natural convection in a closed square region with heat-conducting walls of finite thickness. The obtained results indicate that the thermohydrodynamic parameters differ considerably from the same parameters in the nonconjugate formulation. Aydin [3], using a finite-difference method, analyzed conjugate heat transfer in a double-glazing window (thermal conductivity in only one direction was considered). Optimum thicknesses of the air layer between the glazing layers in a window for various climatic conditions were determined, and the effect of heat-transfer conditions on the boundaries on the thermohydrodynamic state of the object studied was analyzed. Yapici et al. [4] studied conjugate heat transfer in completely developed laminar flow in a channel heated on the outer contour. The channel considered had walls of silicon carbide and contained liquid metals (lithium and sodium). The cases of flow in a channel with constant thermal properties and temperature-dependent properties were analyzed. Characteristic distributions of temperature and thermal stress were obtained. Merrikh and Lage [5] performed a numerical study of natural convection in a closed rectangular region filled with a liquid flowing over several uniformly distributed heat-conducting blocks. The solution region is an analog for both accommodation facilities and typical radio electronic devices. The effect of the number of blocks and their dimensions on the heat transfer process in the enclosure was determined. Polat and Bilgen [6] studied conjugate heat transfer in half-opened cavities (solar collectors, geothermal tanks, electronic chips), in which one of the walls of finite thickness was subjected to thermal flux and the other walls were thermally insulated. Distributions of thermal and hydrodynamic parameters were obtained for various values of the Rayleigh number and the slope of the cavity to the horizon. Qi-Hong Deng and Guang-Fa Tang [7] and Lee and Ha [8] Investigated the influence of a heat-conducting solid at the center of a gas cavity on the heat-transfer process. It was found that the presence of the heat-conducting barrier led to a reduction in the efficiency of convective heat transfer characterized by the average Nusselt number. Numerical simulation of turbulent flow and conjugate heat transfer in a ring gap with a moving heated internal rod was performed by Shehua Huang

[1]Tomsk Polytechnical University, Tomsk 634050. [2]Tomsk State University, Tomsk 634050; Michaelsher@yandex.ru. Translated from Prikladnaya Mekhanika i Tekhnicheskaya Fizika, Vol. 49, No. 6, pp. 69–81, November–December, 2008. Original article submitted March 6, 2007; revision submitted November 13, 2007.

 

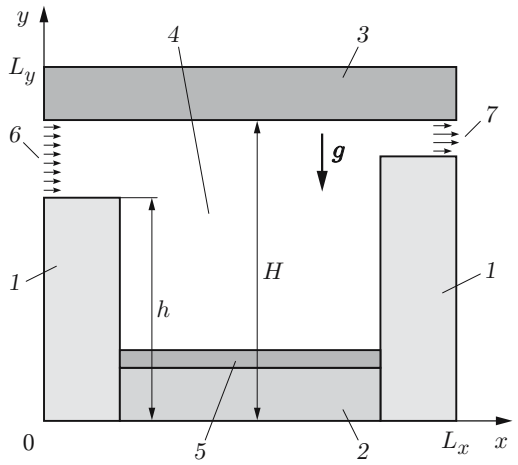


Fig. 1. Solution region of the problem considered: solid blocks (1, 2, and 3), gas cavity (4), heat source (5), entrance hole (6), and exit hole (7).

and Chung-Hwan Chun [9]. The effect of the geometrical parameters of the solution region and the determining dimensionless complexes on the flow and heat transfer conditions was analyzed. Fedorov and Viskanta [10] proposed a model for the thermal state of the microchannel used for heat removal in electronic devices. It was found that the thermal stresses due to high temperature gradients at the entrance into the channel can result in disruption of the heat-removal process.

The papers considered above were focused on finding the regularities of conjugate heat transfer: determining the degree of interrelation between convection in a cavity and heat conduction in the solid wall; estimating the effect of forced and natural flows on the activation of conductive heat transfer; determining the interaction of natural convection (due to the dynamics of conductive heat transfer in solid blocks) and forced flows; determining the role of an external hydrodynamic source in the formation of various flow and heat-transfer regimes. Of greatest interest is to study the evolution of conjugate heat transfer — the origin of free convective flows due to the presence of a temperature gradient in a gas cavity and (or) conductive heat transfer in a solid wall, the interaction of forced and natural convective flows under conditions of high thermal inertia of the solid-wall materials, and the formation of steady-state or quatisteady-state flow regimes.

The present work is a mathematical simulation of mixed gas convection in a rectangular region with solid walls of finite thickness under convective-radiative heat transfer on one of the boundaries with the ambient medium.

**Mathematical Model.** The boundary-value problem of unsteady conjugate heat transfer is considered for the region presented in Fig. 1. The object studied consists of five rectangles which have different dimensions and different thermal characteristic. The temperature of the heat source remains constant throughout the process. The horizontal walls ($y = 0$, $y = L_y$) and the vertical wall ($x = L_x$) of finite thickness which form the gas cavity are assumed to be heat insulated from outside. On the outer boundary $x = 0$, convective-radiative heat transfer with the ambient medium is modeled. The horizontal velocity component at the entrance hole is set constant, and the vertical component is set equal to zero. At the cavity exit, symmetry conditions in the longitudinal direction of the gas flow are specified.

It is assumed that the thermal properties of the solid blocks and gas do not depend on temperature and the flow regime is laminar. The gas is considered incompressible Newtonian fluid which satisfies the Boussinesq approximation.

The heat transfer in the region considered (see Fig. 1) is described by the unsteady two-dimensional equations of convection in the Boussinesq approximation for a gas cavity [14, 15] and the unsteady two-dimensional heat-conduction equation for the solid blocks [16] with nonlinear boundary conditions. The heat transfer due to radiation from the heat source and between the walls is considered negligibly small compared to convective heat transfer and the gas is absolutely transparent to thermal radiation.

The mathematical model is formulated in the dimensionless variables stream function–vorticity–temperature.

The distance scale is taken to be the length of the solution region on the $x$ axis. The system of equations is brought to dimensionless form using the following relations: $X = x/L_x$, $Y = y/L_x$, $\tau = t/t_0$, $U = u/V_{\text{in}}$, $V = v/V_{\text{in}}$, $\Theta = (T - T_0)/\Delta T$, $\Psi = \psi/\psi_0$, $\Omega = \omega/\omega_0$ at $\Delta T = T_{hs} - T_0$, $\psi_0 = V_{\text{in}} L_x$, and $\omega_0 = V_{\text{in}}/L_x$. Here $x$ and $y$ are the Cartesian coordinates, $X$ and $Y$ are the dimensionless coordinates corresponding to the coordinates $x$ and $y$, $t$ is time, $t_0$ is the time scale, $\tau$ is dimensionless time, $u$ and $v$ are projections of the velocity onto the $x$ and $y$ axes, respectively, $U$ and $V$ are the dimensionless velocities corresponding to the velocities $u$ and $v$, $V_{\text{in}}$ is the velocity scale (flow velocity at the cavity entrance), $\Theta$ is the dimensionless temperature, $T_0$ is the initial temperature in the solution region, $T_{hs}$ is the temperature on the surface of the heat source, $\psi$ is the stream function, $\psi_0$ is the scale of the stream function, $\Psi$ is the dimensionless analog of the stream function, $\omega$ is the velocity vortex, $\omega_0$ is scale of the velocity vortex, and $\Omega$ is the dimensionless analog of the velocity vortex.

The conjugate heat transfer is described by the following dimensionless equations:

— for the gas,

$$\frac{\partial \Omega}{\partial \tau} + \frac{\partial \Psi}{\partial Y}\frac{\partial \Omega}{\partial X} - \frac{\partial \Psi}{\partial X}\frac{\partial \Omega}{\partial Y} = \frac{1}{\text{Re}}\,\Delta\Omega + \frac{\text{Gr}}{\text{Re}^2}\,\frac{\partial \Theta}{\partial X}; \tag{1}$$

$$\Delta\Psi = -\Omega; \tag{2}$$

$$\frac{\partial \Theta}{\partial \tau} + \frac{\partial \Psi}{\partial Y}\frac{\partial \Theta}{\partial X} - \frac{\partial \Psi}{\partial X}\frac{\partial \Theta}{\partial Y} = \frac{1}{\text{Re}\,\text{Pr}}\,\Delta\Theta; \tag{3}$$

— for the solid blocks,

$$\frac{1}{\text{Fo}_i}\,\frac{\partial \Theta_i}{\partial \tau} = \Delta\Theta_i, \qquad i = \overline{1,3}. \tag{4}$$

Here $\text{Re} = V_{\text{in}} L_x/\nu$ is the Reynolds number, $\text{Gr} = g_y \beta \Delta T L_x^3/\nu^2$ is the Grashof number, $\beta$ is the temperature coefficient of volume expansion, $g_y$ is the projection of the acceleration due to gravity onto the $y$ axis ($g_x = 0$), $\nu$ is the kinematic viscosity, $\text{Pr} = \nu/a$ is the Prandtl number, $\text{Fo}_i = a_i t_0/L_x^2$ is the Fourier number for the $i$th subregion, $a_i$ is the thermal diffusivity of the $i$th subregion, and $\Delta = \partial^2/\partial X^2 + \partial^2/\partial Y^2$ is the Laplace operator.

For the formulated problem (1)–(4), the initial conditions have the form

$$\Psi(X, Y, 0) = 0, \qquad \Omega(X, Y, 0) = 0, \qquad \Theta(X, Y, 0) = 0.$$

On the heat source, $\Theta = 1$ throughout the process.

In addition, the following boundary conditions are imposed:

1. On the boundary $X = 0$, the conditions taking into account the heat transfer with the ambient medium due to convection and radiation are satisfied:

$$\frac{\partial \Theta_i(X, Y, \tau)}{\partial X} = \text{Bi}_i\,\Theta_i(X, Y, \tau) + \text{Bi}_i\,\frac{T_0 - T_e}{T_{hs} - T_0} + Q_i$$

for

$$Q_i = N_i\Big[\Big(\Theta_i(X, Y, \tau) + \frac{T_0}{T_{hs} - T_0}\Big)^4 - \Big(\frac{T_e}{T_{hs} - T_0}\Big)^4\Big]$$

[$i = 1, 3, 4$ (see Fig. 1)].

2. On the remaining external boundaries, the heat-insulation conditions are specified:

$$\frac{\partial \Theta_i(X, Y, \tau)}{\partial X^k} = 0, \qquad X^1 \equiv X, \quad X^2 \equiv Y, \qquad i = \overline{1,3}.$$

3. In all parts of the solution region in which materials with different thermal characteristics are in contact, conditions of the fourth kind are satisfied:

$$\Theta_i = \Theta_j, \qquad \frac{\partial \Theta_i}{\partial X^k} = \lambda_{j,i}\,\frac{\partial \Theta_j}{\partial X^k}, \qquad i, j = \overline{1,4}, \quad i \neq j, \quad k = 1, 2.$$

4. At the cavity entrance, the energy equation is subject to conditions of the third kind, and the stream function and vorticity are subject to the conditions

$$\Psi = Y - h/L_x, \qquad \Omega = 0.$$

5. The cavity exit is subject to the condition

$$\frac{\partial\Psi}{\partial X} = \frac{\partial\Omega}{\partial X} = \frac{\partial\Theta}{\partial X} = 0.$$

6. On the boundaries between the solid material and the liquid parallel to the $OX$ and $OY$ axes (except on the boundary $Y = H/L_x$), the following conditions are imposed:

$$\Psi = 0, \qquad \frac{\partial\Psi}{\partial Y(\partial X)} = 0, \qquad \Theta_1 = \Theta_4, \qquad \frac{\partial\Theta_1}{\partial Y(\partial X)} = \lambda_{4,1}\,\frac{\partial\Theta_4}{\partial Y(\partial X)}.$$

7. The boundary $Y = H/L_x$ is subject to the conditions

$$\Psi = \frac{H-h}{L_x}, \qquad \frac{\partial\Psi}{\partial Y} = 0, \qquad \Theta_3 = \Theta_4, \qquad \frac{\partial\Theta_3}{\partial Y} = \lambda_{4,3}\,\frac{\partial\Theta_4}{\partial Y}.$$

Boundary condition 7 is obtained from the condition for the velocity at the cavity entrance. Because for $X = 0$, we have $U = 1$ and $V = 0$, in view of $U = \partial\Psi/\partial Y$, we obtain

$$\Psi = \Big(\int\limits_{h/L_x}^{Y} U\,dY\Big)_{U=1} = Y - \frac{h}{L_x},$$

and because on the upper wall, the condition $Y = H/L_x$ is satisfied, it follows that $\Psi = (H-h)/L_x$.

In conditions 1–7, $\mathrm{Bi}_i = \alpha L_x/\lambda_i$ is the Biot number corresponding to the $i$th subregion, $\alpha$ is the coefficient of heat transfer between the ambient medium and the solution region considered, $T_e$ is the ambient temperature, $N_i = \varepsilon\sigma L_x(\Delta T)^3/\lambda_i$ is the Stark number corresponding to the $i$th subregion, $\varepsilon$ is the normalized emissivity factor, $\sigma$ is the Stefan–Boltzmann constant, $\lambda_{ij} = \lambda_i/\lambda_j$ is the relative thermal conductivity, and $\lambda_i$ is the thermal conductivity of the $i$th subregion.

Problem (1)–(4) with the corresponding boundary and initial conditions is solved using a finite-difference method [17, 18]. A uniform difference grid with 20 nodes for the solid blocks and not less than 100 nodes for the gas cavity was used. The results obtained in the present work were obtained on a $200 \times 200$ grid.

Equations (1)–(4) were solved successively. In each time step, we first calculated the temperature field in both the gas cavity and the solid blocks [Eqs. (3) and (4)], then solved the Poisson equation for the stream function (2), then determined the boundary conditions for the vorticity vector using the Woods formula [17, 19], and finally solved Eq. (1).

The convective terms in the evolutionary equations were approximated using the Samarskii monotonic scheme [18] with averaging over $U$ and $|U|$ ($V$ and $|V|$) lest the scheme be independent of the velocity sign. The diffusion terms were discretized by means of central finite differences. Equations (1)–(4) were solved numerically using the locally one-dimensional Samarskii scheme [18] which reduces the solution of the two-dimensional system to a successive solution using the method of marching of one-dimensional systems as systems of difference equations with three-diagonal matrices. The nonlinear boundary condition of the third kind was solved by using simple iterations. The employed locally one-dimensional scheme is absolutely stable, and the approximation of the difference scheme of the initial differential problem has order $O(\tau + h^2 + l^2)$ [18]. The Poisson equation (2) for the stream function was solved in each time step by the relaxation method [17].

The employed solution method has been tested on a number of model problems of both free convective heat transfer and conjugate heat transfer. A comparison of the results obtained in our study with the results of [20, 21] shows that they are in fairly good agreement.

**Results of Numerical Simulation.** Numerical studies of the boundary-value problem (1)–(4) with the corresponding initial and boundary conditions were performed for the following values of the dimensionless complexes characterizing typical regimes of conjugate mixed convection: $\mathrm{Re} = 500$ and 1000, $\mathrm{Gr} = 10^6$, $\mathrm{Pr} = 0.702$, $\mathrm{Bi}_1 = 1.8$, $\mathrm{Bi}_3 = 1.3$, $N_1 = 8.3 \cdot 10^{-5}$, and $N_3 = 6 \cdot 10^{-5}$. The Fourier criterion took the following values depending on the material of the solid blocks: $\mathrm{Fo}_1 = 4.1 \cdot 10^{-5}$, $\mathrm{Fo}_2 = 8.6 \cdot 10^{-6}$, and $\mathrm{Fo}_3 = 3.6 \cdot 10^{-5}$. The dimensionless determining temperatures were $\Theta_e = -1$, $\Theta_{hs} = 1$, and $\Theta_0 = 0$; the temperature complex was $T_0/(T_{hs} - T_0) = 7.325$. The relative thermal conductivities on the interfaces took the following values: $\lambda_{4,1} = 0.037$, $\lambda_{4,3} = 0.026$, and $\lambda_{2,1} = 0.36$.

Since the problem considered is formulated in dimensionless variables, the obtained results can be used in designing various technical devices and equipment in the examined range of determining parameters, which limits the characteristic size of objects to $10^{-2}$–$10^{-1}$ m.

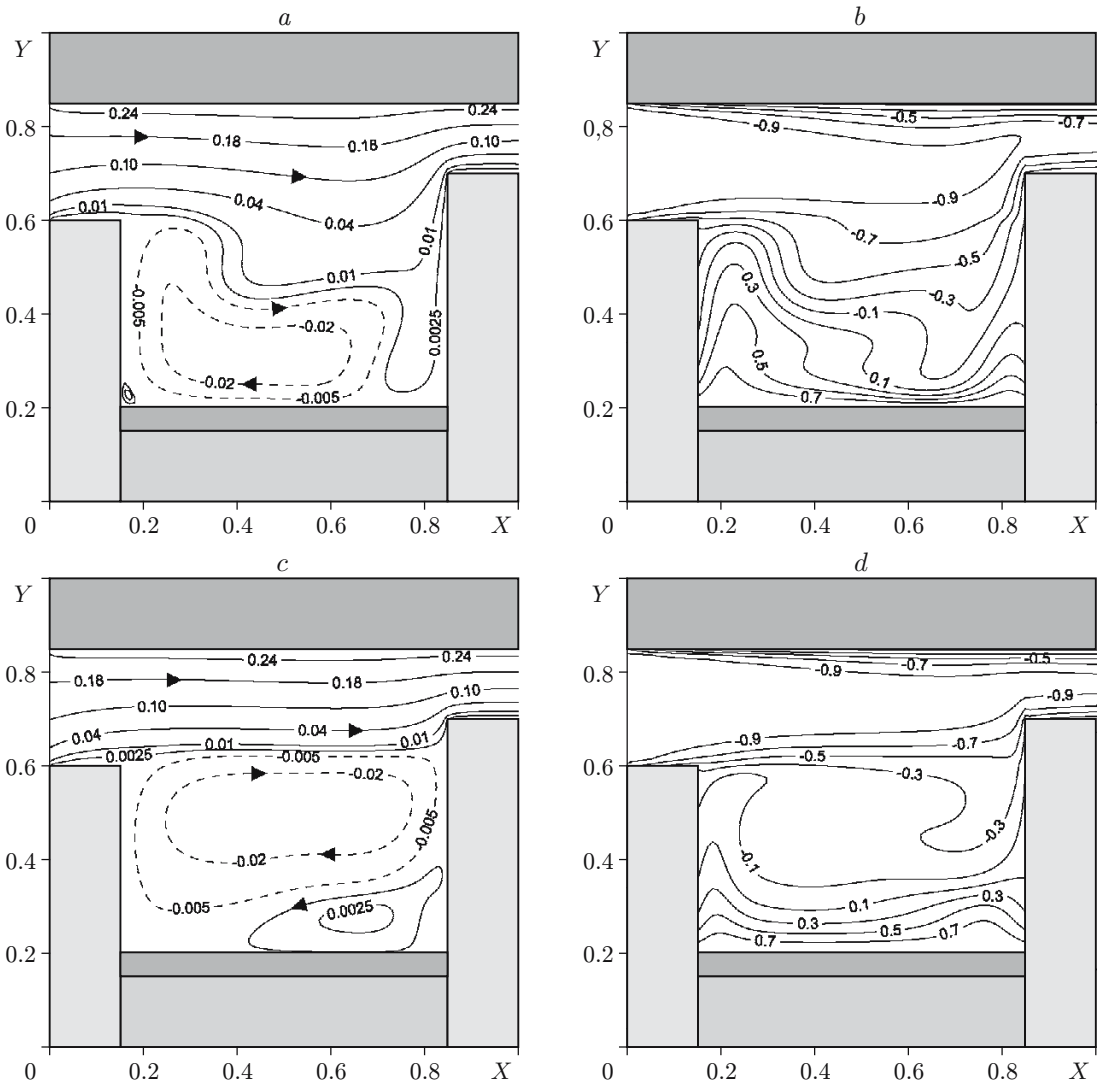


Fig. 2. Streamlines $\Psi$ (a and c) and temperature fields $\Theta$ (b and d) at $\mathrm{Gr} = 10^6$ and $\tau = 100$ with the buoyancy forces taken into account: $\mathrm{Re} = 500$ (a and b) and 1000 (c and d).

Figure 2 shows the streamlines and temperature fields corresponding to the mixed convection regime at $\tau = 100$. The arrows on the streamlines indicate the gas flow direction.

The time considered is not the time at which steady-state flow is formed, although at $\mathrm{Re} = 1000$, a quasisteady-state regime is established because the flow pattern and heat transfer do not change significantly with time. At $\tau = 100$ and $\mathrm{Re} = 500$, the flow regime is not steady-state and continues to evolve, which can be explained by the low velocity of the external flow and, accordingly, the more intense interaction of forced and natural convection.

At $\mathrm{Re} = 500$, a convective cell is formed inside the gas cavity and, due to the influence of the forced flow, this cell is deformed. The corresponding streamline configuration is determined by both the external flow velocity and the geometry of the region. The height of the right wall of the region is greater than the height of the left wall, resulting in the occurrence of descending flows of cold gas near the right wall. Secondary recirculation flows are formed in the corner zones of the gas cavity. The forced flow transfers cold gas rather intensely. This leads to the activation of conductive heat transfer in the solid blocks. The distribution of isotherms in the gas cavity follows the configuration of the flows formed, which indicates the interrelation between hydrodynamics and heat transfer in problems of mixed and natural convection. The absence of symmetry of the temperature field in the left and

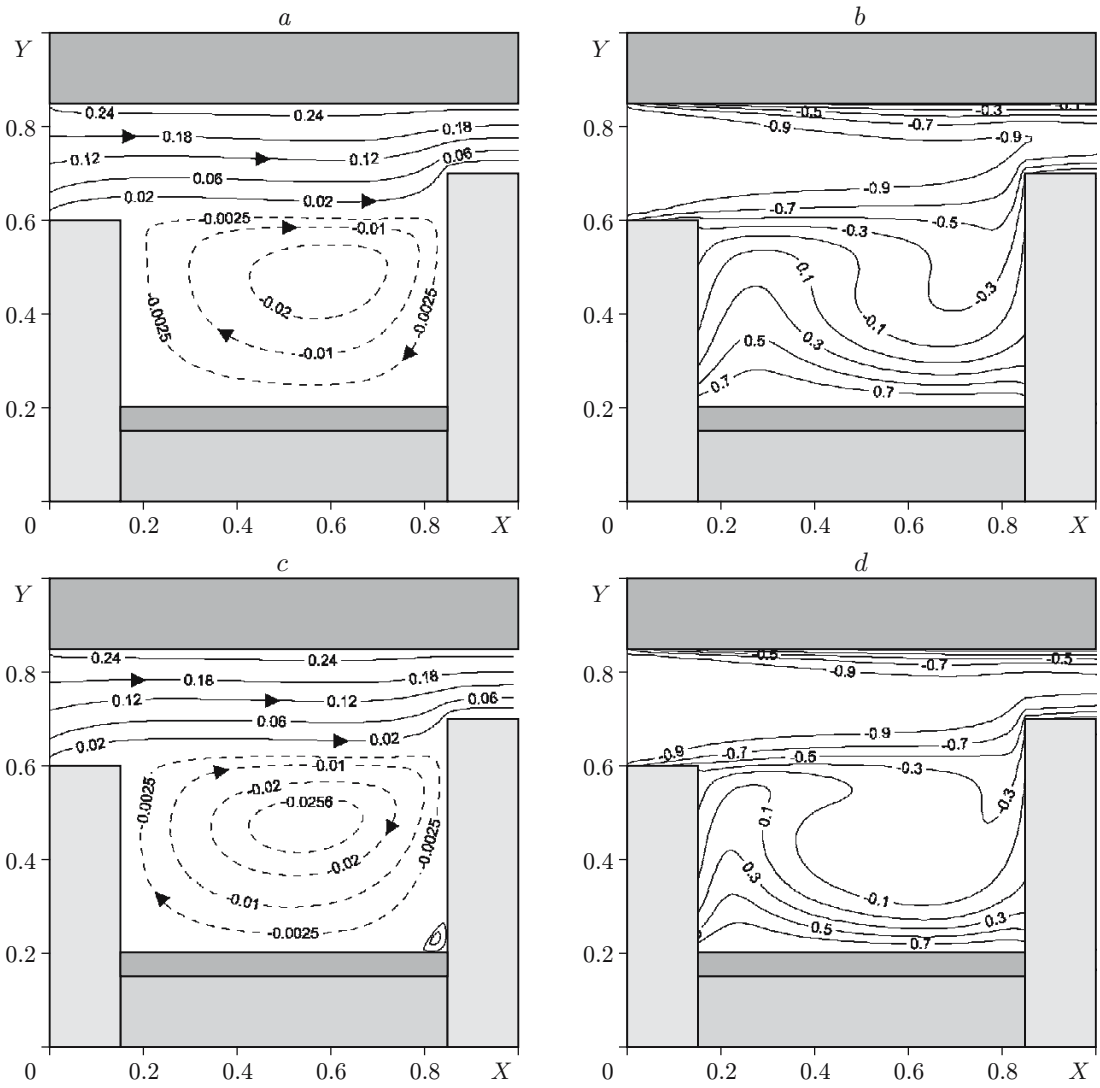


Fig. 3. Streamlines $\Psi$ (a and c) and temperature fields $\Theta$ (b and d) at $\mathrm{Gr} = 10^6$, $\tau = 100$ ignoring buoyancy forces: $\mathrm{Re} = 500$ (a and b) and 1000 (c and d).

right blocks of the solid material in the region of the heater is due to the effect of the ambient medium (convection and radiation on the boundary $X = 0$).

A factor of two increase in the forced flow velocity ($\mathrm{Re} = 1000$) leads to changes in the shape of both the streamlines and the temperature field. Two free convective cells are formed in the gas cavity. The main circulating flow would occupies the larger part of the gas cavity above the heater. The occurrence of secondary flow near the right wall is caused by the propagation of a high-temperature wave from the heat source. The distribution of the isotherms also changes. The interaction of two thermal boundary layers located near the left and right blocks of the solid material leads to the formation of a peculiar conductive core at the center of the gas cavity. In this case, $\mathrm{Re} = 1000$, the average temperature of the gas cavity (from the heat source to the lower boundary of the entrance hole) is higher than that in the case $\mathrm{Re} = 500$.

We analyzed the effect of buoyancy forces on the formation of the flow regimes considered. Figure 3 gives the streamlines and temperature fields corresponding to forced convection [the boundary-value problem (1)–(4) with the same boundary conditions, but in the equation of vortex diffusion, the term defining the role of the buoyancy force is equal to zero: $(\mathrm{Gr}/\,\mathrm{Re}^2)\,\partial\Theta/\partial X = 0$] at $\tau = 100$.

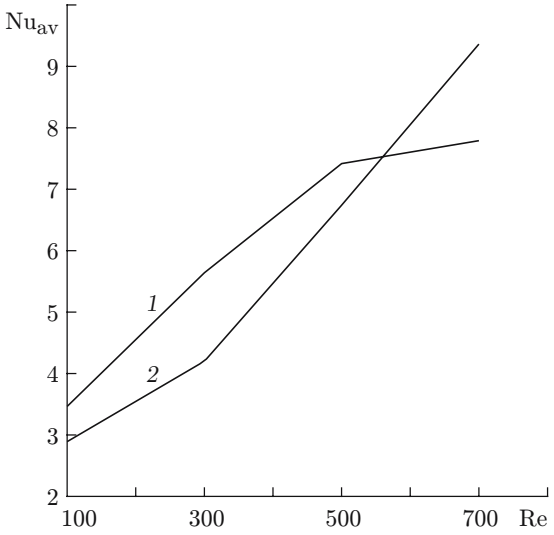


Fig. 4. Average Nusselt number on the boundary $X = 0.85$ versus Reynolds number at $\mathrm{Gr} = 10^6$ and $\tau = 100$ ignoring buoyancy forces (curve 1) and taking into account buoyancy forces (curve 2).

In the convective heat transfer regime (Fig. 3a and b) corresponding to $\mathrm{Re} = 500$, only one convective cell is formed in the gas cavity, which is due to the hydrodynamics of the process. In this case, descending flows are absent near the right block of the solid material. The temperature field also differs from the distribution obtained with the buoyancy force taken into account. The thermal plume above the heat source is more uniform than in the case of the presence of buoyancy forces, where there are significant nonlinear changes in the configuration of isotherms in the region ($0.4 < X < 0.6$; $0.2 < Y < 0.4$).

A factor of two increase in the velocity of the external forced flow (Fig. 3c and d) leads to the formation of a small-scale secondary vortex in the right bottom corner of the gas cavity, whereas in the presence of buoyancy forces above the energy source (see Fig. 2c and d), large-scale recirculation flow is formed. In the case of mixed convection, the thermal plume from the heat source is low (see Fig. 2c and d) whereas in the case of forced convection, it is higher (see Fig. 3c and d).

The above-mentioned differences influence the character of the dependence of the integral heat-transfer coefficient on the boundary $X = 0.85$ on the Reynolds number (Fig. 4)

$$\mathrm{Nu_{av}} = \frac{1}{0.5}\int\limits_{0.2}^{0.7} \Big|\frac{\partial\Theta}{\partial X}\Big|_{X=0.85} dY = f(\mathrm{Re}).$$

The influence of unsteadiness on the distributions of thermal and hydrodynamic characteristics was analyzed with and without accounting for buoyancy forces (Figs. 5 and 6, respectively). Figure 5 gives the streamlines and temperature fields corresponding to the flow regime at $\mathrm{Re} = 1000$ and $\mathrm{Gr} = 10^6$ for various times.

At $\tau = 20$ (see Fig. 5a and b) five convective cells are formed in the gas cavity, which bock the forced flow to some extent, displacing it to the upper block of the solid material. The occurrence of such convective cells is due to an instantaneously arising temperature gradient in the cavity since the ambient medium was motionless at the initial time although the source temperature was set maximal.

In convective flows, a determining factor is the quantity $\mathrm{Gr}/\mathrm{Re}^2$ [14], which characterizes the ratio of natural and forced convection. For small values of $\mathrm{Gr}/\mathrm{Re}^2$, the process is determined by forced convection and for large values, it is determined by natural convection. For intermediate values which corresponds to the problem considered, mixed convection is the case.

In Fig. 5a and b, it is evident that, at $\tau = 20$, the temperature field only begins to form. Isotherms propagate nonuniformly from the heat source, which is due to the influence of forced flow. In turn, external flow leads to the propagation of low temperature to the gas cavity.

If buoyancy forces are ignored (see Fig. 6a and b), one convective cell is formed in the gas cavity. In this case, the thermal plume propagates uniformly from the heat source.

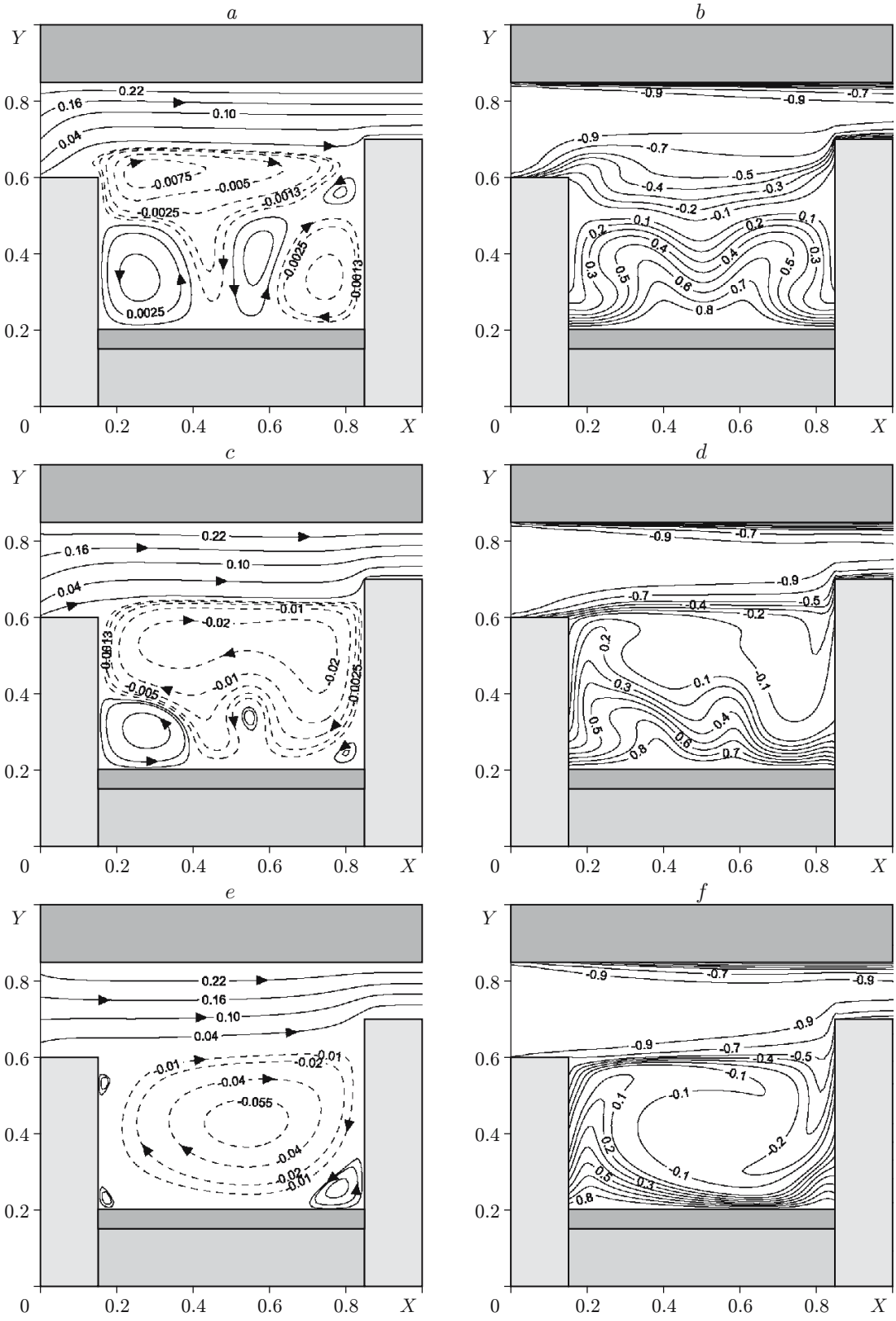


Fig. 5. Streamlines $\Psi$ (a, c, and e) and temperature fields $\Theta$ (b, d, and f) at $\mathrm{Re} = 1000$ and $\mathrm{Gr} = 10^6$ with buoyancy forces taken into account: $\tau = 20$ (a and b), 60 (c and d), and 600 (e and f).

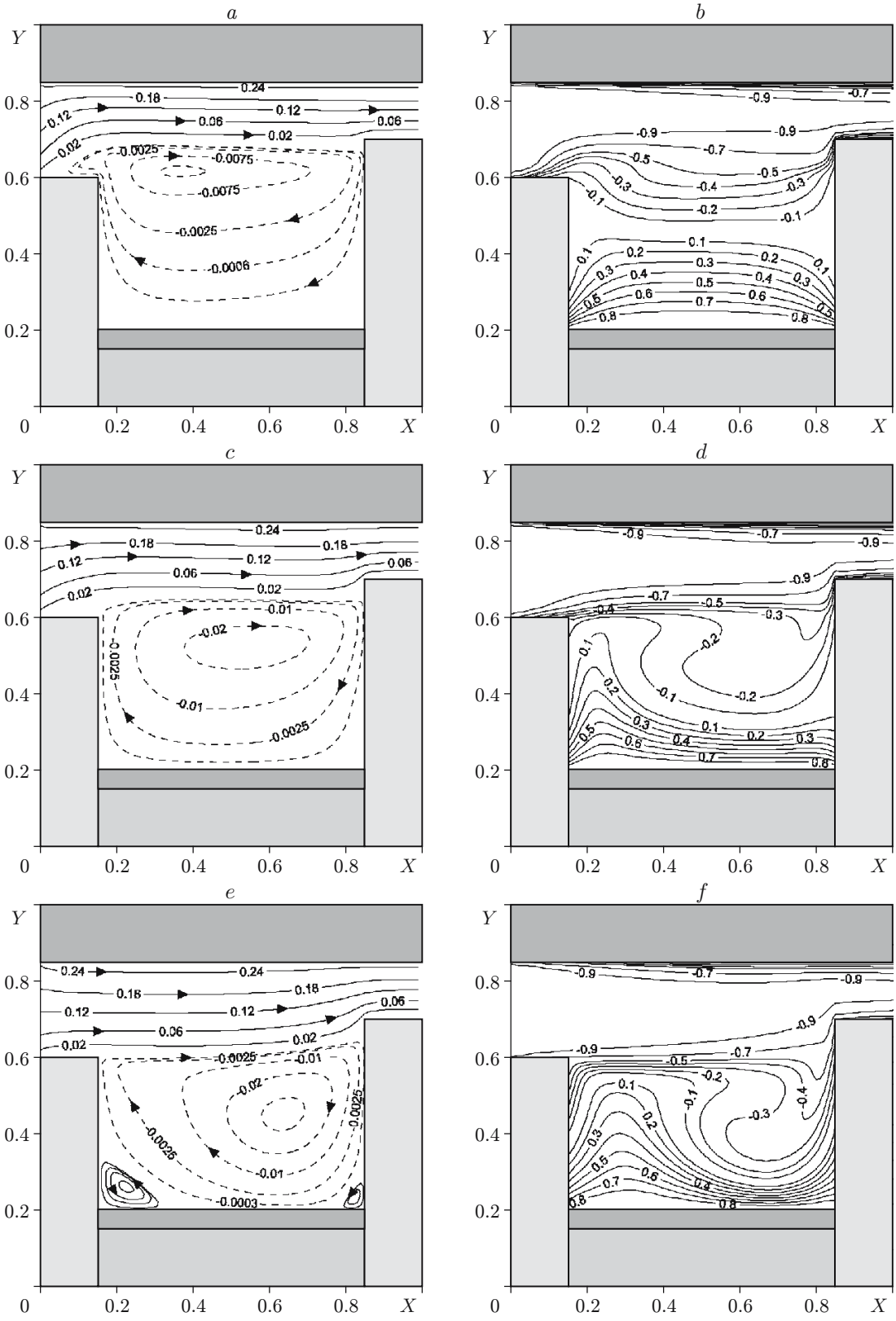


Fig. 6. Streamlines $\Psi$ (a, c, and e) and temperature fields $\Theta$ (b, d, and f) at $\mathrm{Re} = 1000$ and $\mathrm{Gr} = 10^6$ ignoring buoyancy forces: $\tau = 20$ (a and b), 60 (c and d), and $\tau = 600$ (e and f).

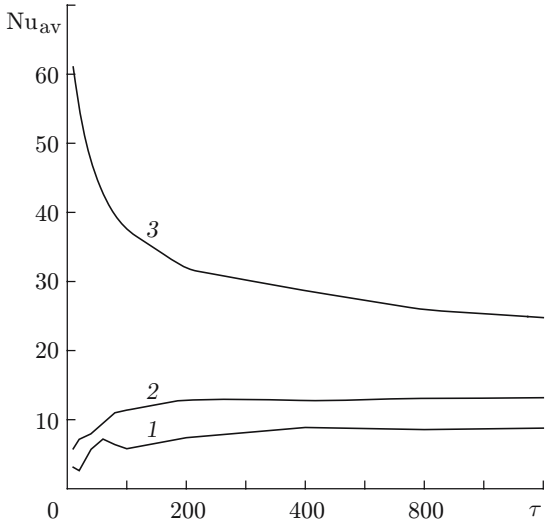


Fig. 7. Average Nusselt number versus time at Re = 1000, Gr = $10^6$ with buoyancy forces taken into account: curves 1, 2, and 3 refer to $Nu_1$, $Nu_2$, and $Nu_3$, respectively.

A factor of three increase in the time interval ($\tau = 60$) leads to a considerable change in both the flow pattern and temperature field (see Fig. 5c and d). In the gas cavity there are absorption and blocking of some vortices, resulting in a decrease in their scales or dissipation. The symmetry in the distribution of the isotherms is broken, and the thermal plume is shifted to the left wall. The activation of the forced flow leads to the motion of the cold wave front in the solid blocks.

In the case of forced convection (see Fig. 6c and d), only one convective cell remains in the gas cavity. The temperature field is formed under the influence of two currents — a warm ascending current and a cold descending current. During the interaction between the thermal plume from the heat source and the jet from the entrance hole, the nonmonotonic portions of the isotherms that are seen in Fig. 5c and d are not formed.

Further increase in $\tau$ (see Fig. 5e and f) leads to integration of the vortex structures into one circulating flow with the retention of the secondary recirculations caused by both the geometry of the region and the examined flow regime. The temperature field also changes: a quasisteady-state temperature field is formed in the gas cavity due to the interaction of two boundary layers.

In the case of no buoyancy forces (see Fig. 6e and f) the flow pattern and the temperature field also change.

The influence of unsteadiness on the average Nusselt number was analyzed on three interfaces between the gas cavity and the solid blocks (Fig. 7):

$$\mathrm{Nu}_1 = \frac{1}{0.4}\int\limits_{0.2}^{0.6} \left|\frac{\partial\Theta}{\partial X}\right|_{X=0.15} dY, \quad \mathrm{Nu}_2 = \frac{1}{0.5}\int\limits_{0.2}^{0.7} \left|\frac{\partial\Theta}{\partial X}\right|_{X=0.85} dY, \quad \mathrm{Nu}_3 = \int\limits_{0}^{1} \left|\frac{\partial\Theta}{\partial Y}\right|_{Y=0.85} dX.$$

It is evident that the values of the dimensionless heat-removal coefficient on the three interfaces between the gas cavity and the solid blocks differ significantly.

In the initial region ($0 \leqslant \tau \leqslant 100$), the values of $Nu_1$ change nonmonotonically. This region corresponds to the formation of a thermal regime. As noted above, at $\tau = 100$ a quasisteady-state regime of flow and heat transfer is formed (see Fig. 7).

The values of $Nu_2$ increase monotonically, except in the region $\tau \approx 400$, in which the generalized heat-removal coefficient decreases only slightly, which can be explained by the characteristic features of the process studied. The increase of $Nu_2$ is due to the presence of descending cold gas currents near the right wall, resulting in an increase in the temperature gradient.

The values of $Nu_3$ decrease monotonically because of the gradual cooling of the upper block of the solid material and, hence, a decrease in the temperature gradient at the interface with the gas medium.

**Conclusions.** The problem of mixed convection in a gas cavity was solved numerically for the case of a local heat source and forced flow under radiation-convective heat transfer with the ambient medium. The characteristic

features of the flow and heat transfer for values of the determining parameters $Gr = 10^6$ and $Re = 500$ and 1000 were obtained. It was found that buoyancy forces have a significant effect on the formation of various regimes of convective heat transfer. The unsteadiness factor is shown to influence both local characteristics (streamlines and isotherms) and integral characteristic (the average Nusselt number on three characteristic boundaries). The evolution of the process was found to be due not only to the time-varying effect of the ambient medium but also to the thermal inertia of the solid blocks.

This work was supported by the Russian Foundation for Basic Research (Grant No. 05-02-98006 competition r_Ob_a) and Administration of the Tomsk Region.

## REFERENCES

1. A. V. Lykov, A. A. Aleksashenko, and V. A. Aleksashenko, *Conjugate Problems of Convective Heat Transfer* [in Russian], Nauka Tekhnika, Minsk (1971).
2. A. Liaqat and A. Baytas, "Conjugate natural convection in a square enclosure containing volumetric sources," *Int. J. Heat Mass Transfer*, **44**, No. 17, 3273–3280 (2001).
3. O. Aydin, "Conjugate heat transfer analysis of double pane windows," *Build. Environ.*, **41**, No. 2, 109–116 (2006).
4. H. Yapici, G. Basturk, and B. Albayrak, "Numerical study on conjugate heat transfer in laminar fully developed flow with temperature dependent thermal properties through an externally heated SiC/SiC composite pipe and thermally induced stress," *Energ. Conv. Manage.*, **46**, No. 4, 633–654 (2005).
5. A. A. Merrikh and J. L. Lage, "Natural convection in an enclosure with disconnected and conducting solid blocks," *Int. J. Heat Mass Transfer*, **48**, No. 7, 1361–1372 (2005).
6. O. Polat and E. Bilgen, "Conjugate heat transfer in inclined open shallow cavities," *Int. J. Heat Mass Transfer*, **46**, No. 9, 1563–1573 (2003).
7. Qi-Hong Deng and Guang-Fa Tang, "Numerical visualization of mass and heat transport for conjugate natural convection/heat conduction by streamline and heatline," *Int. J. Heat Mass Transfer*, **45**, No. 11, 2373–2385 (2002).
8. J. R. Lee and M. Y. Ha, "A numerical study of natural convection in a horizontal enclosure with a conducting body," *Int. J. Heat Mass Transfer*, **48**, No. 16, 3308–3318 (2005).
9. Shehua Huang and Chung-Hwan Chun, "A numerical study of turbulent flow and conjugate heat transfer in concentric annuli with moving inner rod," *Int. J. Heat Mass Transfer*, **46**, No. 19, 3707–3716 (2003).
10. A. G. Fedorov and R. Viskanta, "Three-dimensional conjugate heat transfer in the microchannel heat sink for electronic packaging," *Int. J. Heat Mass Transfer*, **43**, No. 3, 399–415 (2000).
11. P. Rajesh Kanna and Manab Kumar Das, "Conjugate forced convection heat transfer from a flat plate by laminar plane wall jet flow," *Int. J. Heat Mass Transfer*, **48**, No. 14, 2896–2910 (2005).
12. B. Abourida and M. Hasnaoui, "Numerical study of partitions effect on multiplicity of solutions in an infinite channel periodically heated from below," *Energ. Conv. Manage.*, **46**, No. 17, 2697–2717 (2005).
13. M. El Alami, M. Najam, E. Semma, et al., "Electronic components cooling by natural convection in horizontal channel with slots," *Energ. Conv. Manage.*, **46**, No. 17, 2762–2772 (2005).
14. Y. Jaluria, *Natural Convection: Heat and Mass Transfer*, Pergamon Press (1980).
15. Yu. A. Sokovishin and O. G. Martyneneko, *Introduction to the Theory of Free Convective Heat Transfer* [in Russian], Izd. Leningrad. Univ., Leningrad (1982).
16. A. V. Lykov, *Theory of Heat Conduction* [in Russian], Vysshaya Shkola, Moscow (1967).
17. V. M. Paskonov, V. I. Polezhaev, and L. A. Chudov, *Numerical Simulation of Heat and Mass Transfer* [in Russian], Nauka, Moscow (1984).
18. A. A. Samarskii, *Theory of Difference Schemes* [in Russian], Nauka, Moscow (1977).
19. E. L. Tarunin, *Computational Experiment in Free-Convection Problems* [in Russian], Izd. Irkutsk. Univ., Irkutsk (1990).
20. G. de. Vahl Davis, "Natural convection of air in a square cavity: A bench numerical solution," *Int. J. Numer. Methods Fluids*, **3**, No. 3, 249–264 (1983).
21. D. A. Kaminski and C. Prakash, "Conjugate natural convection in a square enclosure effect of conduction on one of the vertical walls," *Int. J. Heat Mass Transfer*, **29**, No. 12, 1979–1988 (1986).